Technical Note

Automatic Correction of Echo-Planar Imaging (EPI) Ghosting Artifacts in Real-Time Interactive Cardiac MRI Using Sensitivity Encoding

Yoon-Chul Kim, MS,* Jon-Fredrik Nielsen, PhD, and Krishna S. Nayak, PhD

Purpose: To develop a method that automatically corrects ghosting artifacts due to echo-misalignment in interleaved gradient-echo echo-planar imaging (EPI) in arbitrary oblique or double-oblique scan planes.

Materials and Methods: An automatic ghosting correction technique was developed based on an alternating EPI acquisition and the phased-array ghost elimination (PAGE) reconstruction method. The direction of k-space traversal is alternated at every temporal frame, enabling lower temporal-resolution ghost-free coil sensitivity maps to be dynamically estimated. The proposed method was compared with conventional one-dimensional (1D) phase correction in axial, oblique, and double-oblique scan planes in phantom and cardiac in vivo studies. The proposed method was also used in conjunction with two-fold acceleration.

Results: The proposed method with nonaccelerated acquisition provided excellent suppression of ghosting artifacts in all scan planes, and was substantially more effective than conventional 1D phase correction in oblique and double-oblique scan planes. The feasibility of real-time reconstruction using the proposed technique was demonstrated in a scan protocol with 3.1-mm spatial and 60-msec temporal resolution.

Conclusion: The proposed technique with nonaccelerated acquisition provides excellent ghost suppression in arbitrary scan orientations without a calibration scan, and can be useful for real-time interactive imaging, in which scan planes are frequently changed with arbitrary oblique orientations.

Key Words: echo-planar imaging (EPI); ghosting artifacts; echo-misalignment; real-time interactive MRI; sensitivity encoding (SENSE)
J. Magn. Reson. Imaging 2008;27:239–245.
© 2007 Wiley-Liss, Inc.

ECHO-PLANAR IMAGING (EPI) (1) is used in cardiac MRI because it accelerates image acquisition, while maintaining image quality comparable to two-dimensional Fourier transform (2DFT). Cardiac EPI often introduces artifacts in reconstructed images, which may include geometric distortion and ghosting due to a variety of sources including off-resonance, in-plane flow, cardiac motion, and echo-misalignment. Geometric distortions due to off-resonance can be mitigated by reducing the echo spacing in the readout gradient or acquiring the data using multiple radio frequency (RF) excitations (i.e., shots), which increases the effective sampling rate (i.e., increases the acquisition bandwidth) along the phase-encode direction. Ghosting due to in-plane flow and cardiac motion can be mitigated by making the acquisition faster or restricting data acquisition to a relatively stationary cardiac phase.

Ghosting artifacts caused by echo-misalignment are a systemic problem, and are a function of induced eddy currents and system timing errors, which are associated with the scanner hardware (e.g., eddy currents from the cryostat and relative delays of the physical x, y, and z gradients). These issues are further complicated in oblique scan planes, which are routinely used in real-time imaging (e.g., cardiac short-axis and long-axis views).

The conventional method for correcting echo-misalignment involves performing a calibration scan to determine the on-axis gradient/data acquisition (DAQ) time delays, and using small gradient "blips" to align echoes. These blips are scan-plane–dependent (2,3), and should be redesigned upon each scan-plane change. Flyback readouts (4), which involve acquiring data only on the positive polarity of the readout gradient, can be used to avoid echo-misalignment artifacts without a calibration scan, but have the disadvantage of reduced scan time efficiency. Image-based correction (5), which takes into account one-dimensional (1D) phase errors from reduced field of view (FOV) images reconstructed separately from odd and even echoes, is effective at reducing ghosting artifacts in on-axis scan planes, but its effectiveness may be degraded in oblique (and double-oblique) scan planes. Full 2D correction is possible using fully phase-encoded reference scans for each scan plane (6), but it may be impractical to acquire such reference scans in dynamic and/or real-time imaging applications. Furthermore, use of such 2D phase-error maps may be problematic when imaging rapidly

moving structures such as the heart, in which the estimated phase-error between odd and even echoes will be biased by phase-accrual due to flow and motion.

Another alternative is to separate data from left-to-right and right-to-left traversals in k-space (which each have half the desired FOV), and to reconstruct ghost-free full-FOV images using parallel imaging (7–10). This approach is attractive for real-time imaging because it does not require additional calibration scans or any modification of the pulse sequences at the time of scan plane change. The phased-array ghost elimination (PAGE) method (9) has provided a generalized framework for canceling ghosting artifacts due to sources including off-resonance and echo-misalignment using the information of local coil sensitivity profiles from multiple coils. Herzka et al (8) demonstrated gated cardiac imaging with a sequential noninterleaved EPI acquisition scheme, in which the echo-train-length (ETL) was equal to the sensitivity encoding (SENSE) reduction factor (e.g., 2 or 3).

In this work, we propose an "interleaved" gradient-echo EPI acquisition scheme and associated reconstruction method. Compared to the original PAGE method, this acquisition uses a large ETL ranging from 15 to 50 and a small number of shots to achieve sufficient temporal resolution in free-breathing real-time cardiac EPI imaging. Using shot-to-shot interleaving of the phase-encode lines and a "double-alternating" k-space data acquisition scheme, the proposed method achieves ghost suppression using a SENSE reduction factor of 2, regardless of the ETL. The proposed technique is compared with the conventional 1D phase correction method (5) in oblique and double-oblique scan planes. Two-fold accelerated EPI imaging is also demonstrated in conjunction with the proposed automatic ghosting correction technique. Finally, the feasibility of real-time reconstruction is demonstrated using a custom real-time imaging platform (11).

MATERIALS AND METHODS

When performing EPI at oblique or double-oblique scan planes, two or all three physical gradients will oscillate during each readout. An important consideration is that physical gradients in x, y, and z may have unequal delays (2). For an oblique scan plane with unequal gradient delays, the k-space lines with different traversal directions in the logical coordinate frame will sample positions in k-space that are shifted in opposite directions along the physical coordinate axes. Combined data are not uniformly spaced, which causes artifacts in reconstructed images. Within the set of lines having the same traversal direction, uniform spacing is maintained.

The proposed acquisition scheme involves acquiring k-space data with alternating polarity of the readout gradient. Figure 1a illustrates the proposed reconstruction method. Coil sensitivity maps are reconstructed separately from the left-to-right (L-R) and right-to-left (R-L) lines, which are acquired from the two most recent time frames, N and N–1 (12). The L-R and R-L lines each preserve uniform spacing between phase encode lines and prevent artifacts due to echo-misalignment (8). In

time frame N, SENSE (13) reconstruction with a reduction factor of 2 is applied separately to the L-R and R-L lines. The resulting two full-FOV images differ not in magnitude but in phase, and taking a root sum-of-squares combination eliminates distortions in phase and recovers signal-to-noise ratio (SNR). This nonaccelerated double-alternating scheme can be applied to any number of interleaves as long as L-R and R-L lines are alternating along the phase encode. An even number of interleaves would require that the phase-encode blips alternate in size.

Figure 1b illustrates that automatic EPI ghosting correction and two-fold acceleration can be achieved simultaneously by controlling interleaf order as shown. In this case, full-FOV coil sensitivity maps are estimated on the fly based on four adjacent time frames. After separating L-R and R-L data, a reduction factor of 4 can be used to perform SENSE unaliasing operations. In general, to perform accelerated imaging with the proposed method and an acceleration factor of $A \geq 2$, the SENSE reconstruction will require a reduction factor of $2A$, which must not exceed the total number of coils, and the most recent $2A$ time frames will be used for forming coil-sensitivity maps. The accelerated method can be applied to double-alternating EPI with oA interleaves for any odd integer o using phase-encode blips with constant size, and with eA interleaves for any even integer e using phase-encode blips with alternating size.

1D phase correction (5) is used for comparison in the phantom and in vivo studies because it also does not rely on any calibration, and is compatible with real-time imaging. For each coil, a 1D phase map representing constant and linear phase errors is computed using phase differences between the L-R and R-L images. 1D phase correction is performed using Eq. [12] from Ref. 5. A root-sum-of-squares operation is performed to produce the final corrected image, with the images from all coils considered for reconstruction.

Experiments were performed on a Signa Excite 3 T scanner (GE Healthcare, Waukesha, WI, USA) with gradients capable of 40 mT/m amplitudes and 150 mT/m/msec slew rates. The receiver bandwidth was set to ± 125 kHz, i.e., 4 μsec sampling time. The body coil, capable of peak B_1 of 16 μT, was used for RF transmission and an eight-channel cardiac array coil was used for signal reception.

Circular EPI (CEPI) trajectories (14), which have a circular k-space footprint, were designed in MATLAB (The Mathworks, South Natick, MA, USA). CEPI trajectories used in the experiments produced a 10% to 15% reduction in readout duration compared to conventional rectangular EPI trajectories. A bipolar pulse was added to the phase encode gradient waveform prior to data acquisition to null the first moment in the y direction at $k_y = 0$. Alternating interleaved EPI readouts with an odd number of interleaves were used (15,16), and this k-space traversal pattern was flipped in the readout direction at every time frame. Echo-time shifting (17) was used to mitigate off-resonance effects.

Real-time interactive cardiac scanning was performed using the RTHawk real-time imaging platform (11). Scan planes were changed interactively by the operator to test
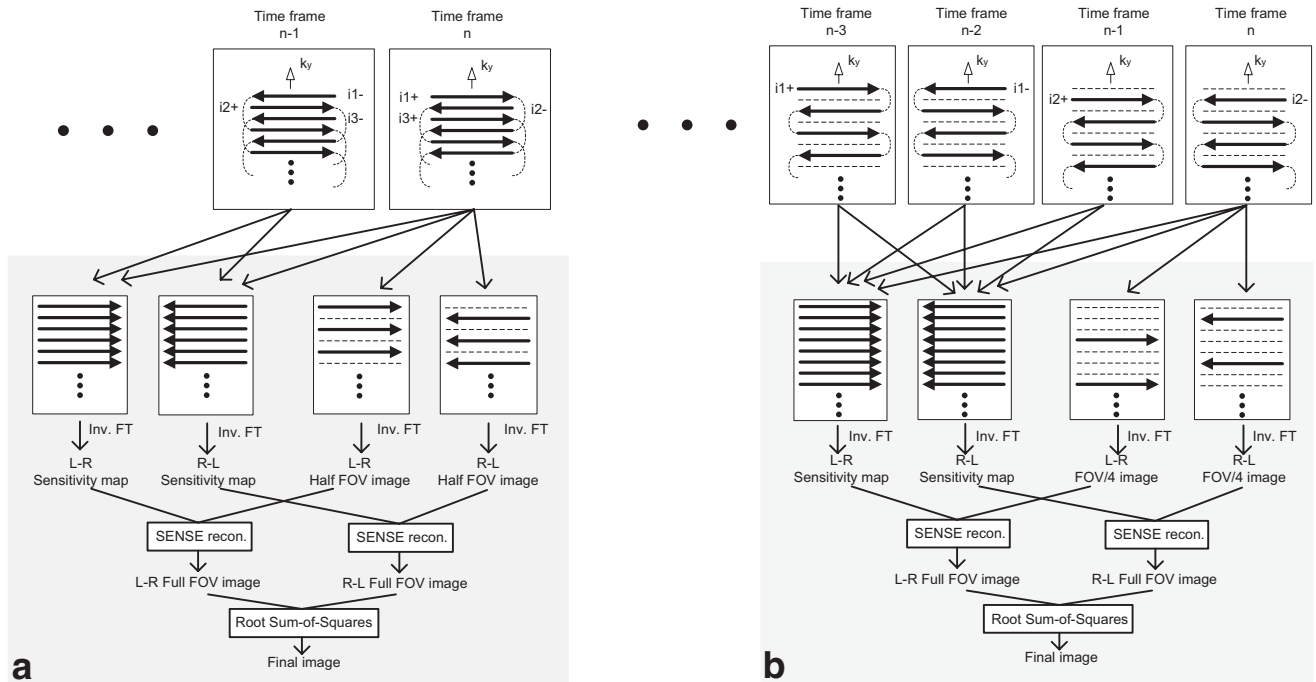
Figure 1. Reconstruction flowchart for the proposed ghosting correction method for (**a**) nonaccelerated and (**b**) two-fold–accelerated EPI with automatic ghosting correction. a: The acquisition and reconstruction as a function of time is shown for three-interleaves, and can be applied to any odd number of interleaves with constant phase-encode blip size, or to any even number of interleaves with an alternating phase-encode blip size. At time frame $N–1$, a full k-space dataset is acquired with the interleaf ordering: i1–, i2+, i3–. At time frame N, another full dataset is acquired with ordering: i1+, i2–, i3+. These two sets are repeated continuously. Note that "–" indicates that the readout gradient is flipped. To reconstruct a ghost-free image for time frame N, L-R data lines and R-L data lines are separated. The most recent two temporal frames are used to form coil sensitivity maps separately from L-R and R-L full-FOV data (middle row). SENSE reconstruction is used to form full-FOV L-R and R-L images for the current time frame, which are then combined using root-sum-of-squares, to produce a final image representing time frame N. b: When accelerating data acquisition time by a factor of 2, a SENSE reduction factor of four is needed. The most recent four temporal frames are used to form coil sensitivity maps. In general, if a reduction factor of R can be achieved for a particular coil geometry and scan planes, it can be combined with the proposed EPI strategy with an acceleration factor of R/2 since one-half of the reduction factor is used for separating L-R and R-L lines during reconstruction and the remainder can still be used for acceleration.

the performance of the proposed method at all angles. A spectral-spatial RF pulse was used to excite water spins, with a 5.2-mm slice thickness, and 440-Hz bandwidth (18). Flip angles of 15–25° were used. The proposed reconstruction was performed both off-line and on-line, and videos were produced off-line. Raw data from all four anterior receiver channels were used to perform SENSE reconstruction in the nonaccelerated acquisition, and raw data from all eight elements were used to perform SENSE reconstruction in the accelerated case. The noise correlation matrix used in SENSE reconstruction was computed using the formula presented in the Appendix section of Ref. 13 from raw data obtained with the RF excitation turned off.

Phantom experiments were conducted to quantitatively evaluate the level of ghost suppression. A cylindrical phantom was imaged with axial, oblique, and double-oblique scan orientations. The proposed method was compared with conventional 1D phase correction (5). The effectiveness of ghost suppression was evaluated by comparing ghost-to-signal ratios (GSR) within the same manually-selected region of interest (ROI).

Cardiac in vivo experiments were performed on three healthy volunteers without gating or breathholding,

and were evaluated qualitatively. Each subject was screened and provided informed consent in accordance with institutional policy.

The nonaccelerated automatic ghosting correction method was implemented in C++, within the RTHawk real-time reconstruction software (11). The LAPACK linear algebra package was used for the matrix inversion operations required during SENSE reconstruction. A Linux personal computer (Compaq R3000) with a single 3.2-GHz Intel central processing unit (CPU) and 896-MB random access memory (RAM) was used for real-time reconstruction. Data were sent from the host computer to the reconstruction computer via Ethernet after each TR (11). Reconstruction time was measured separately using the built-in C++ "gettimeofday" function for the following four reconstruction steps: 1) coil sensitivity map estimation, 2) aliased image reconstruction, 3) SENSE matrix inversion, and 4) image display.

RESULTS

In all figures, the readout and phase encode directions correspond to the horizontal and vertical axes, respec-
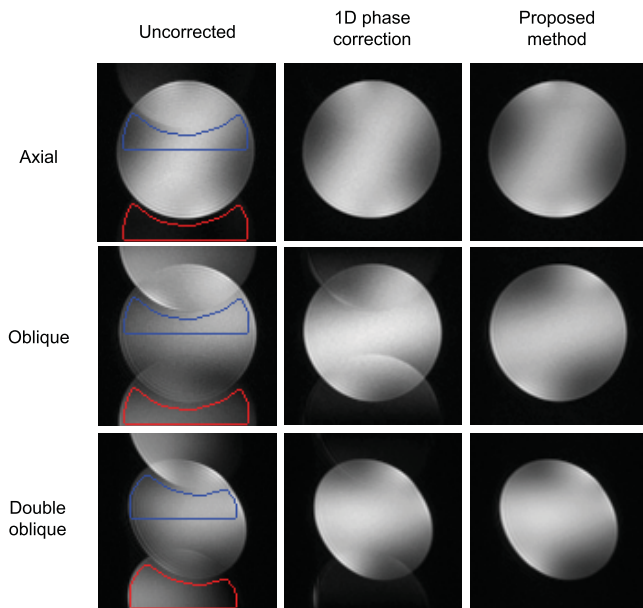
Figure 2. Real-time cylindrical phantom images reconstructed with nonaccelerated EPI data. Data from four receiver coils (two from anterior and the other two from posterior receiver coils) in the eight-channel cardiac array coil were used for reconstruction. Reconstruction results for axial (top row), oblique (middle row), and double-oblique (bottom row) scan planes are shown using no correction, 1D phase correction, and the proposed correction method. The blue and red contours, superimposed on uncorrected images, represent ROIs for signal and ghost, respectively. The pixel values in the ROIs were used to compute GSRs. Images reconstructed with the proposed method are ghost-free even in oblique and double-oblique scan planes. Scan parameters: double-alternating CEPI with five interleaves, ETL = 19, FOV = 21 × 21 cm^2, spatial resolution = 2.2 × 2.2 mm^2, TR = 39 msec, and time-per-image = 195 msec.

tively. The uncorrected images in Figs. 2 and 3 were reconstructed by performing an inverse Fourier transform of the raw data without separating the L-R and R-L acquisitions, and without applying any postprocessing method for EPI ghosting correction.

Figure 2 contains phantom images reconstructed from data acquired in axial, oblique, and double-oblique scan planes. Both 1D phase correction and the proposed method produce visually comparable ghost-free images in the axial scan plane. However, in oblique and double-oblique scan planes, ghosting artifacts are prominent when using conventional 1D phase correction but are significantly reduced when using the proposed method. GSR values are listed in Table 1 and demonstrate the effectiveness of the proposed method. The GSRs for oblique and double-oblique scan planes for the proposed method were 3.40% and 2.03%, respectively, whereas those for 1D phase correction were 8.76% and 6.18%, respectively. The mean and standard deviation (SD) of g-factor values for the proposed method are also listed in Table 1. The average g-factor values ranged from 1.2 to 1.3 in all three scan planes considered.

Figure 3 contains in vivo cardiac images for four standard cardiac views in one representative volunteer. Un-

corrected images are shown alongside images reconstructed using 1D phase correction and the proposed method. Uncorrected images exhibit ghosting artifacts in all four cardiac views, and are most severe in the two-chamber and four-chamber views. Both 1D phase correction and the proposed method produce appreciable suppression of ghost artifacts in all views. The proposed method produces better image quality and improved ghost suppression compared to 1D phase correction (indicated by white arrows in Fig. 3). However, the proposed method experiences noise amplification due to the use of parallel imaging with a reduction factor of 2. The mean and SD of g-factor values were 1.45 ± 0.50, 1.75 ± 0.94, 1.34 ± 0.33, and 1.34 ± 0.28, for the axial, two-chamber, four-chamber, and short-axis views, respectively.

Figure 4 illustrates a double-oblique short-axis view during rapid scan-plane rotation. The scan plane was
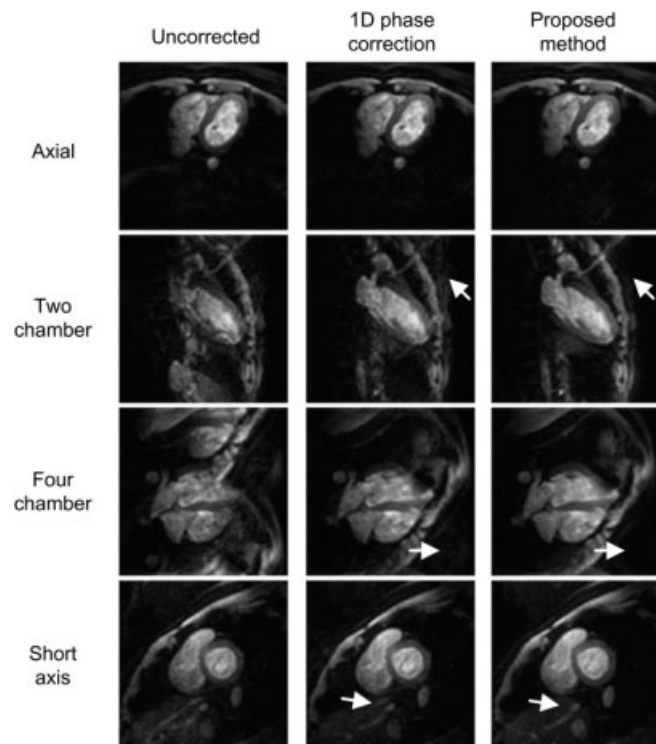
Figure 3. In vivo real-time cardiac images reconstructed with nonaccelerated EPI data. Data from four anterior receiver coils in the eight-channel cardiac array coil were used for reconstruction. Uncorrected (left column), 1D phase corrected (middle column), and corrected images with the proposed correction scheme (right column) are shown for four standard views: axial, two-chamber, four-chamber, and short-axis. Ghosting artifacts are substantially reduced in all four corrected images with the proposed method. The white arrows indicate that residual ghosting artifacts are clearly visible in images reconstructed with the 1D phase correction method, but they are not observed in images reconstructed with the proposed method. See also Movie 1 of the supplementary material available online at http://www.interscience.wiley.com/jpage/1053-1807/suppmat/index.html. Scan parameters: double-alternating CEPI with three interleaves, ETL = 27, FOV = 25 × 25 cm^2, spatial resolution = 3.1 × 3.1 mm^2, TR = 20 msec, and time-per-image = 60 msec.

Table 1
GSR from the Phantom Study (See Fig. 2) for 1D Phase Correction and the Proposed Method*

Scan plane	1D phase correction	Proposed method	
	GSR (%)	GSR (%)	g-Factor (mean ± SD)
Axial	3.94	4.24	1.26 ± 0.25
Oblique	8.76	3.40	1.28 ± 0.28
Double oblique	6.18	2.03	1.27 ± 0.26

*Mean ± SD of g-factor values for the proposed method are also reported.

rotated in increments of 10° continuously throughout the acquisition. Ghosting artifacts are suppressed even during rapid changes in scan orientation. Note that images at 0.9, 1.2, and 3.3 seconds appear blurred because they occur during scan plane changes.

Figure 5 compares two-fold acceleration with no acceleration and also illustrates the effect of motion on low temporal resolution coil sensitivity maps. Coil sensitivity maps were reconstructed using either: data temporally adjacent to the target data (scheme I), or data obtained from a stable diastolic phase (scheme II).

An FOV of 33 cm (rather than 25 cm) was used to mitigate the g-factor increase when using a reduction factor of 4 with our eight-element cardiac array. Two-fold accelerated images (Fig. 5c and h) exhibit much lower SNR than nonaccelerated images (Fig. 5b and g) because of the reduced acquisition time and the highly elevated g-factor. In some areas the g-factor reached 10 (Fig. 5e). Coil sensitivity maps obtained using calibration scheme I exhibit motion induced ghosting artifacts (Fig. 5a, solid arrow), while those obtained using calibration scheme II exhibit substantially reduced motion
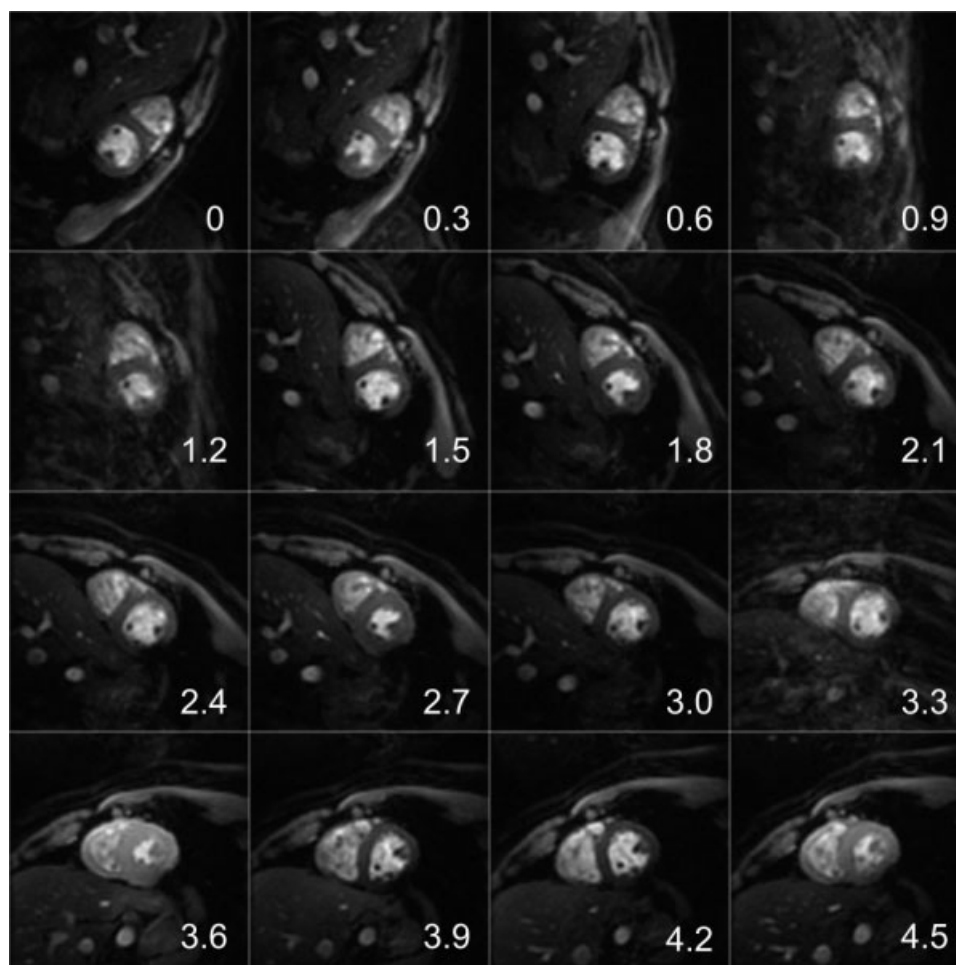
Figure 4. Automatic correction during continuous scan plane rotation. Scan parameters were identical to those described in Fig. 3. Reconstructed images using the proposed method are shown with respect to time. Numbers in the lower right corners in the images denote time in seconds. The interval between images is 300 msec, which corresponds to a spacing of five time frames. Note the decrease in contrast between myocardium and blood during the systolic phase in the cardiac cycle (see images at 3.6 and 4.5 seconds). See also Movie 2 of the supplementary material available online at http://www.interscience.wiley.com/jpages/1053-1807/suppmat/index.html.
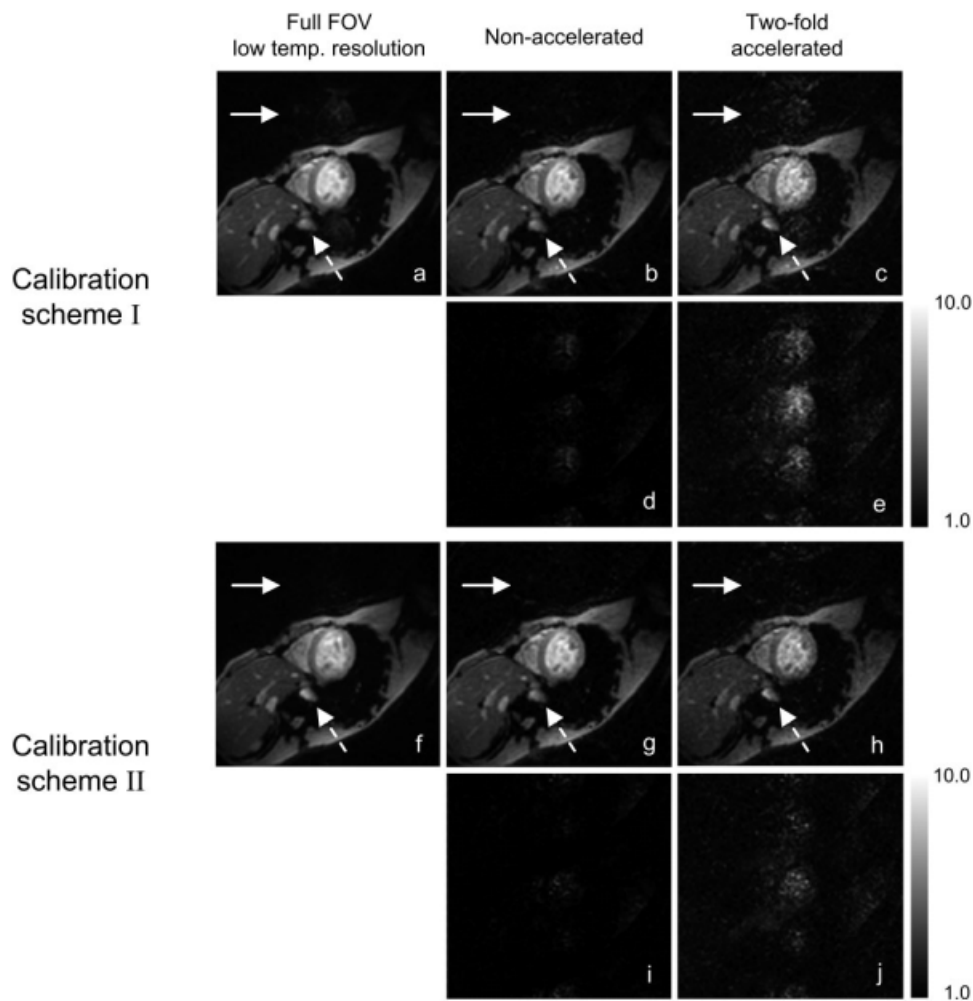
Figure 5. Automatic ghosting correction using no acceleration (**b**, **g**) and two-fold acceleration (**c**, **h**) and their corresponding g-factor maps (**d**, **i**, **e**, **j**) reconstructed using two coil calibration schemes, I and II. Full FOV images (**a**) with low temporal resolution are used for coil calibrations. The target data are from a systolic cardiac phase in which cardiac motion is substantial. g-Factor maps are shown using a scale from 1 to 10. Note that g-factor values from calibration scheme II (**i, j**) are significantly lower than those from calibration scheme I (**d, e**), especially for the two-fold accelerated case. Motion artifacts are noticeably reduced for the two-fold accelerated case when using calibration scheme II (solid arrows). Two-fold accelerated images have lower SNR because of reduced acquisition time and the elevated g-factor, but show less temporal blurring in the descending aorta (dashed arrows) compared to nonaccelerated images. See also Movie 3 of the supplementary material available online at http://www.interscience.wiley.com/jpages/1053-1807/suppmat/index.html. Scan parameters: double-alternating CEPI with two interleaves, ETL = 50, FOV = 33×33 cm^2, spatial resolution = 3.3×3.3 mm^2, TR = 34 msec, and time-per-image = 136 msec (full FOV low temporal resolution for coil calibration), 68 msec (nonaccelerated), and 34 msec (two-fold accelerated).

artifacts (Fig. 5f, solid arrow). Ghosting artifacts in the coil sensitivity maps lead to residual ghosting in the final images (Fig. 5b and c, compared to Fig. 5g and h). The mean and SD of g-factor values were 1.25 ± 0.37 and 2.05 ± 0.90 for the nonaccelerated and two-fold accelerated cases, respectively, using calibration scheme I, and were 1.16 ± 0.25 and 1.79 ± 0.58 for the nonaccelerated and two-fold accelerated cases, respectively, using calibration scheme II. Two-fold accelerated images exhibit less temporal blurring of structures because of the reduced acquisition time (e.g., descending aorta indicated by dashed arrows).

Reconstruction time for the nonaccelerated method was measured for the real-time reconstruction algorithm. Average run time measurements for the different reconstruction steps were: 45.04 msec for the compu-

tation of coil sensitivity maps, 41.45 msec for the computation of aliased images, 57.44 msec for SENSE matrix inversion operations, and 0.84 msec for image display. The total reconstruction time was approximately 144 msec per frame, while the acquisition time per image was 60 msec. This indicates that pipelining this computation across three processors will be sufficient for real-time reconstruction using commercially available personal computer hardware.

DISCUSSION

The proposed method effectively eliminated ghosting artifacts due to EPI echo-misalignment in arbitrary double-oblique scan planes. When applied to real-time interactive imaging, it automatically corrected ghosting

artifacts without a calibration scan whenever a scan plane change occurred. This automatic capability is attributed to the fact that ghost-free coil sensitivity maps are updated with a few recent time frames, e.g., two time frames for the nonaccelerated acquisition and four time frames for the two-fold accelerated acquisition. In this method, a factor of 2 in SENSE reduction is used solely for correcting EPI ghosting artifacts, and not for accelerating data acquisition. In the nonaccelerated acquisition, in which a SENSE reduction factor of two is used, noise amplification due to the SENSE matrix inversion was relatively insignificant. However, in the two-fold accelerated acquisition, in which a SENSE reduction factor of four is used, the SENSE noise amplification was severe. This can be mitigated by using 16-channel, 32-channel, or larger receiver coil arrays for which rate-4 parallel imaging has been demonstrated with reasonable g-factors (19).

A drawback of the proposed method is that lower temporal resolution coil sensitivity maps suffer from motion induced ghosting artifacts when cardiac motion occurs during coil calibration. Coil sensitivity maps corrupted with motion artifacts produce residual artifacts in final corrected images. A simple way of alleviating this effect is to use the data from a relatively stationary diastolic cardiac phase to construct coil sensitivity maps that are free from motion induced ghosting. In our experiments, the use of stationary frames for coil calibration substantially reduced ghosting artifacts in final corrected images. Alternatively, the use of temporal low-pass filtering in coil calibration may also mitigate ghosting artifacts in coil sensitivity maps (12).

When the nonaccelerated correction method was applied to real-time cardiac imaging at 3T, overall reconstructed images demonstrated high temporal resolution, excellent suppression of ghosting artifacts, and high blood–myocardium contrast. In systolic cardiac phases, subtle but noticeable FOV/2 ghosting was observed due to rapid cardiac motion. In end-diastolic cardiac phases, almost no ghosting was observed. While three-interleaf gradient-echo EPI was primarily used, we also experimented with other odd numbers of interleaves. Single-shot EPI was considered as a way to further accelerate acquisition, but signal loss and blurring due to T_2^* relaxation proved to be limiting, given the same spatial resolution as the imaging protocol used in Fig. 3. The use of five or more interleaves increased the prevalence of artifacts due to cardiac motion and the lowered temporal resolution.

In conclusion, an interleaved gradient-echo EPI acquisition strategy, and PAGE-based reconstruction technique have been presented as a means for automatically correcting EPI ghosting artifacts due to echo misalignment. The method was applied successfully to real-time interactive cardiac imaging at 3T, with superior performance compared to conventional 1D correction. Ghosting artifacts were automatically corrected at arbitrary oblique scan planes, and high-quality ghost-free images were obtained with 3.1-mm spatial resolu-

tion and 60-msec temporal resolution. The automatic EPI ghosting correction method utilizes parallel imaging with a reduction factor of 2, and may also be compatible with further acceleration using higher reduction factors when 16, 32, or higher channel receiver coil arrays are used. The feasibility of real-time reconstruction using commercially available workstations was demonstrated.

REFERENCES

1. Mansfield P. Multi-planar image formation using NMR spin echoes. J Phys C 1977;10:L55–L58.
2. Reeder SB, Atalar E, Faranesh AZ, McVeigh ER. Referenceless interleaved echo-planar imaging. Magn Reson Med 1999;41:87–94.
3. Zhou X, Epstein FH, Maier JK. Reduction of a new Nyquist ghost in oblique echo planar imaging. In: Proceedings of the 4th Annual Meeting of ISMRM, New York, NY, USA, 1996 (Abstract 1477).
4. Feinberg DA, Turner R, Jakab PD, Kienlin MV. Echo-planar imaging with asymmetric gradient modulation and inner-volume excitation. Magn Reson Med 1990;13:162–169.
5. Buonocore MH, Gao L. Ghost artifact reduction for echo-planar imaging using image phase correction. Magn Reson Med 1997;38:89–100.
6. Chen N-K, Wyrwicz AM. Removal of EPI Nyquist ghost artifacts with two-dimensional phase correction. Magn Reson Med 2004;51:1247–1253.
7. Kuhara S, Kassai Y, Ishihara Y, Yui M, Hamamura Y, Sugimoto H. A novel EPI reconstruction technique using multiple RF coil sensitivity maps. In: Proceedings of the 8th Annual Meeting of ISMRM, Denver, CO, USA, 2000 (Abstract 154).
8. Herzka DA, Kellman P, Aletras AH, Guttman MA. Multishot EPI-SSFP in the heart. Magn Reson Med 2002;47:655–664.
9. Kellman P, McVeigh ER. Phased array ghost elimination. NMR Biomed 2006;19:352–361.
10. Griswold MA, Jakob PM, Edelman RR, Sodickson DK. Alternative EPI acquisition strategies using SMASH. In: Proceedings of the 6th Annual Meeting of ISMRM, Sydney, Australia, 1998 (Abstract 423).
11. Santos JM, Wright GA, Pauly JM. Flexible real-time magnetic resonance imaging framework. Conf Proc IEEE Eng Med Biol Soc 2004;2:1048–1051.
12. Kellman P, Epstein FH, McVeigh ER. Adaptive sensitivity encoding incorporating temporal filtering (TSENSE). Magn Reson Med 2001;45:846–852.
13. Pruessmann KP, Weiger M, Scheidegger MB, Boesiger P. SENSE: sensitivity encoding for fast MRI. Magn Reson Med 1999;42:952–962.
14. Pauly JM, Butts RK, Luk Pat GT, Macovski A. A circular echo planar pulse sequence. Proceedings of the 3rd Annual Meeting of SMR, Nice, France 1995:106.
15. Buonocore MH, Zhu DC. High spatial resolution EPI using an odd number of interleaves. Magn Reson Med 1999;41:1199–1205.
16. Hennel F. Image-based reduction of artifacts in multishot echo-planar imaging. J Magn Reson 1998;134:206–213.
17. Feinberg DA, Oshio K. Gradient-echo shifting in fast MRI techniques for correction of field inhomogeneity errors and chemical shift. J Magn Reson 1992;97:177–183.
18. Nayak KS, Cunningham CH, Santos JM, Pauly JM. Real-time cardiac MRI at 3 Tesla. Magn Reson Med 2004;51:655–660.
19. Hardy CJ, Harvey EC, Giaquinto RO, Niendorf T, Grant AK, Sodickson DK. 32-element receiver-coil array for cardiac imaging. Magn Reson Med 2006;55:1142–1149.